Published in final edited form as:

Balos, V., Marekha, B. A., Malm, C., Wagner, M., Nagata, Y., Bonn, M., et al. (2019). Specific Ion Effects on an Oligopeptide: Bidentate binding matters for the Guanidinium Cation. Angewandte Chemie International Edition in English, 58(1), 332-337. doi:10.1002/anie.201811029.

Supporting Information

Specific Ion Effects on an Oligopeptide: Bidentate binding matters for the Guanidinium Cation

Vasileios Balos, Bogdan Marekha, Christian Malm, Manfred Wagner, Yuki Nagata, Mischa Bonn and Johannes Hunger

Specific Ion Effects on an Oligopeptide: Bidentate binding matters for the Guanidinium Cation

Vasileios Balos,[a,b] Bogdan Marekha,[a] Christian Malm,[a] Manfred Wagner,[a] Yuki Nagata,[a] Mischa Bonn[a] and Johannes Hunger[a]*

[a] *Max Planck Institute for Polymer Research, Ackermannweg 10, 55128 Mainz, Germany*
[b] *Present address: Fritz Haber Institute of the Max Planck Society, Faradayweg 4, 14195 Berlin, Germany*
** Email: hunger@mpip-mainz.mpg.de*

Supporting Information

Materials

Triglycine (BioUltra ≥ 99% Sigma Aldrich) and the salts KCl (Sigma Aldrich), KI (Sigma Aldrich), KSCN (Sigma Aldrich), LiCl (Sigma Aldrich) and GdmCl (Sigma Aldrich), were used as received. Three different series of solutions were prepared volumetrically: (a) series of aqueous triglycine solutions, which were prepared at concentrations, c_{GGG}, between 0.05 to 0.3 mol·L^{-1} at increments of 0.05 mol·L^{-1}, (b) ternary solutions of triglycine (0.247 mol·L^{-1}) + water + salt with increasing concentrations of salt, c_{salt}, at 0.05, 0.1, 0.2, 0.3, 0.4, 0.5, 0.6 and 0.75 mol·L^{-1}. These samples were prepared by diluting an aqueous stock solution with a given mass fraction of triglycine with concentrated aqueous salt stock solutions and water. (c) for NMR experiments ternary solutions of triglycine (0.5 mg·mL^{-1}) + D_2O + salt, with the salt concentrations scaling at molar ratios (of triglycine:salt) of 1:0, 1:1, 1:5, 1:10, 1:50, 1:100, 1:500 and 1:1000 were prepared by mixing solutions of salt in D_2O and triglycine in D_2O.
To avoid uptake of moisture, all salt stock solutions of series (b) and (c) were prepared by weighing the appropriate amount of salt in a glove box and subsequently adding Milli-Q water or D_2O (Eurisotope 99.90 % D).

Experimental Methods

Complex permittivity spectra were measured using a combination of two different experiments: We cover frequencies at $0.2 \leq \nu/GHz \leq 36$ by using a frequency domain reflectometer based on Anritsu Vector Star MS4647A, vector network analyser with an open ended coaxial probe, based on 1.85 mm coaxial connectors.[1] Frequencies at $56 \leq \nu/GHz \leq 125$ were covered analogously using an open ended coaxial probe, based on 1 mm coaxial connectors together with an external frequency converter module (Anritsu 3744A mmW module).
To obtain the molar concentration of triglycine in the stock solution we measured its density using a DM45 DeltaRange density meter apparatus from Mettler Toledo.
Dynamic viscosity, η, of the samples of series (a) were determined using a capillary Ubbelohde viscometer (ViskoSystem AVS 370, Schott Instruments, Germany).
^{1}H-NMR experiments were performed on a 850 MHz Bruker AVANCE III system equipped with a 5 mm triple resonance TXI ^{1}H/^{13}C/^{15}N probe with a z-gradient. For proton NMR 512 transients using a 9 µs long 90° pulse and a 17000 Hz spectral width together with a recycling delay of 5 s. For referencing a sealed capillary with DMSO-d_6 was placed inside the 5 mm tube with a small fraction of DMSO-d_5H. The temperature was controlled to 298.3 K with a VTU (variable temperature unit) and an accuracy of +/- 0.1 K and calibrated with a standard ^{1}H methanol NMR sample using the Topspin 3.1 software (Bruker).

Dielectric relaxation of aqueoeus Triglycine solutions

We fit the relaxation model described in the main manuscript (eq. 1) to the spectra of all binary samples. The thus extracted parameters for different concentrations of GGG are summarized in Figs. S1 and S2.

From the extracted amplitudes of the dielectric relaxation of triglycine, S_{GGG}, we obtain the effective dipole moment of GGG, $\mu_{\mathrm{eff,GGG}}$, which is shown in Fig. 1c of the main manuscript using the Cavell relation:[2]

$$S_{\mathrm{GGG}} = \frac{\varepsilon_{\mathrm{s}}}{\varepsilon_{\mathrm{s}} + (1-\varepsilon_{\mathrm{s}})/3} \cdot \frac{N_{\mathrm{A}} c_{\mathrm{GGG}}}{3 k_{\mathrm{B}} T \varepsilon_0} \cdot \mu^2_{\mathrm{eff,GGG}} \qquad \text{(S1)}$$

,where N_A is the Avogadro's number, k_B the Boltzmann's constant, ε_0 the permittivity of free space, and T the thermodynamic temperature. ε_{s} is the static dielectric permittivity of the samples (see also eq. 1; $\varepsilon_{\mathrm{s}} = S_{\mathrm{GGG}} + S_{\mathrm{water}} + \varepsilon_\infty$).

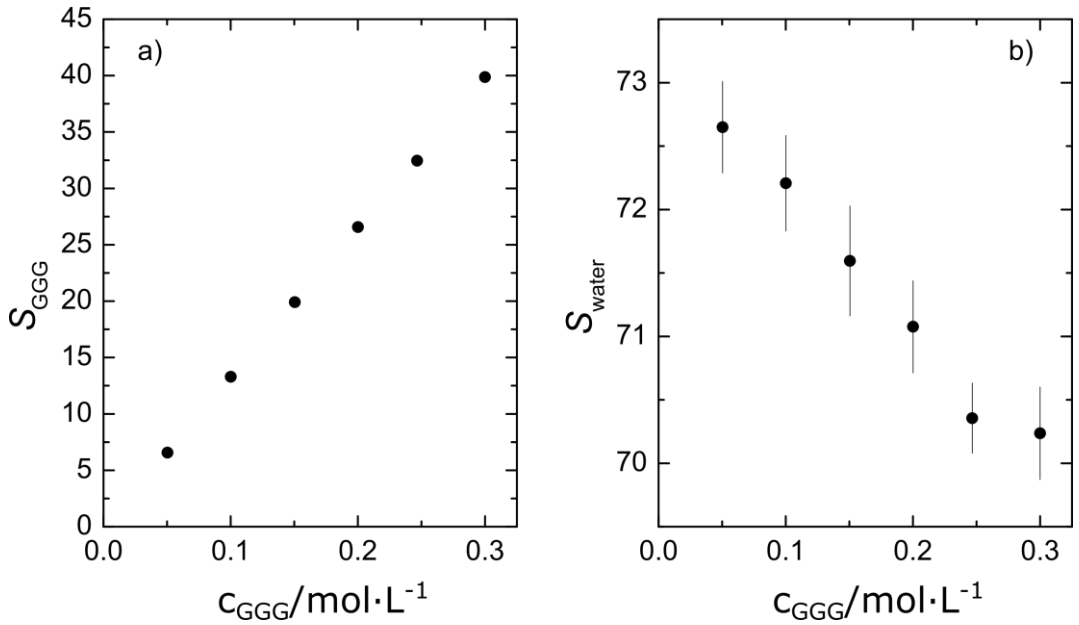

Figure S1. Relaxation amplitudes of a) triglycine (S_{GGG}) and b) water (S_{water}), as obtained by fitting eq.1 to the dielectric spectra of aqueous solutions of GGG. The error bars correspond to the standard deviation within six independent measurements.

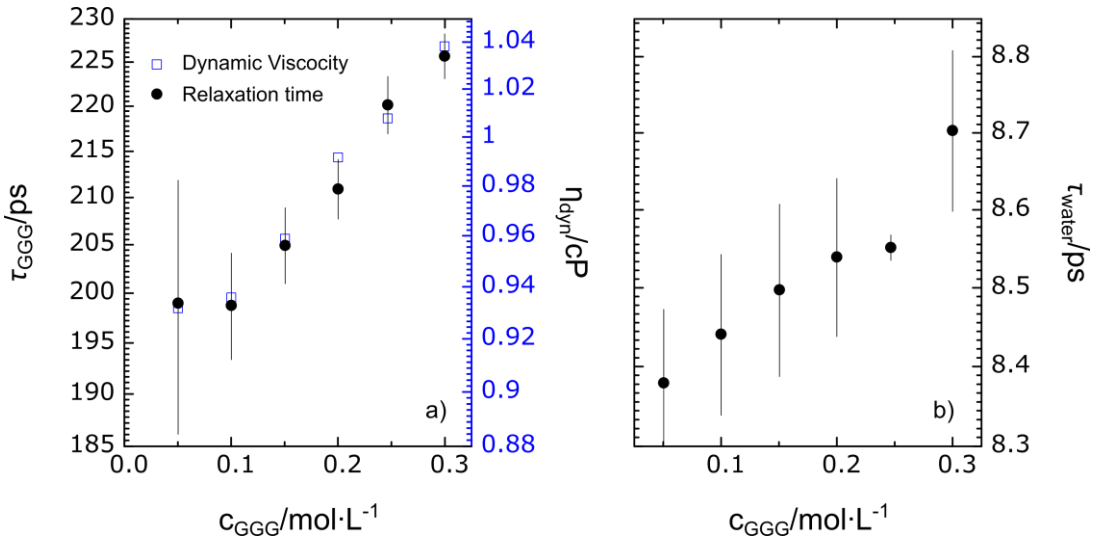

Figure S2. a) Relaxation times of triglycine, $\boldsymbol{\tau_{GGG}}$, (black solid squares) together with the dynamic viscosity, $\boldsymbol{\eta_{dyn}}$, of the samples (blue open squares) and b) relaxation time of water ($\boldsymbol{\tau_{water}}$) as a function of triglycine concentration as obtained from fitting eq.1 to the experimental data. The error bars correspond to the standard deviation within six independent measurements.

Molecular dynamics simulation details

All-atom simulations were performed with NAMD 2.12[3] code using the latest release of the CHARMM C36m additive force-field for GGG and ions in combination with CHARMM modified TIP3P water model.[4,5] We selected the classical CHARMM force-field due to its well-known transferability[4] and also because GGG was among the benchmark peptide set used to adjust the backbone dihedral energy terms against experimental *J*-coupling values.[5]

Initial structures were prepared with the Molefacture plugin of the VMD 1.9.3 software.[6] An uncapped GGG zwitterion in a fully stretched conformation (often referred to as β-sheet like or polyglycine I[7]) was placed in the center of a cubic simulation box with 5 nm side length and solvated with either neat TIP3P water or 1 mol·L^{-1} LiCl, KCl or GdmCl (75 ion pairs).

Standard three-dimensional periodic boundary conditions were employed. Non-bonded Lennard-Jones and electrostatic interactions were explicitly calculated at each time step between atoms within $r_{cut\text{-}off}$ = 1.2 nm distance. The former were smoothly brought to zero at $r_{cut\text{-}off}$ together with the corresponding forces using a switching function at separation distances between 1.0 and 1.2 nm. The neglected long-range contribution to the Lennard-Jones energy term and virial has been accounted for via the corresponding correction.[8] Long-range (reciprocal) part of the electrostatic interactions was computed using the particle mesh Ewald (PME)[9] scheme with charges interpolated on a grid with a spacing of approximately 0.1 nm using fifth order B-splines. Neighbour lists for the non-bonded interaction calculation were updated every 20 simulation steps to include atoms within 1.4 nm distance, while the interactions between atoms separated by one or two bonds were excluded and Lennard-Jones interactions between atoms separated by three bonds were scaled according to the CHARMM scheme.[5] All bond lengths involving hydrogen atoms were kept fixed by means of the SHAKE algorithm[10] whereas water molecules were maintained rigid using the SETTLE method[11], which allowed for the use of 2 fs time step with the velocity Verlet integrator.[12]

The systems were first energy minimized using conjugate gradients method for 5000 steps. They were then subject to 110 ns long constant temperature (300 K) and pressure (1 atm) simulations. The temperature was maintained using Langevin thermostat with the damping coefficient of 5 ps^{-1} while the pressure was controlled via the Langevin piston Nosé-Hoover method[13,14] as implemented in NAMD with the Langevin piston period of 100 fs and 50 fs decay time. The first 10 ns of the trajectories were discarded as equilibration period and 25000 equally time spaced frames were taken for analysis from the last 100 ns.

In order to confirm that the simulation length employed in the present study is sufficient to sample the relevant conformational states of GGG we calculated the relative Gibbs free energy maps of the two-dimensional probability distribution of the Ramachandran (φ, ψ) backbone dihedral angles of the central Gly residue (Fig. S3). Similar distributions were already reported by Best et al.[5] for C-term protonated GGG from a 400 ns long equilibrium run and by Drake and Montgomery Pettitt[15] for C- and N-term capped GGG from a 300 ns long trajectory both using C36m force-field and similar simulation set up.
Despite the differences in the termini (fully charged in the present work, partially charged,[5] or capped[15]), our results are in excellent agreement with literature reports,[5,15] since differences in terminal capping and C-term protonation are not expected to have an impact on the Ramachandran distributions of the central residue as long as N-term is not deprotonated.[16] In particular, we observe essentially equal populations of the right- and left-handed α-helical regions at (−/+ 75 °; −/+ 30 °) which are about 1.5 kcal mol^{-1} less stable than a partially extended polyglycine II (PG II) conformation observed around (± 70 °; ± 150 °) while the fully extended polyglycine I conformation (PG I or β) at (± 150 °; ± 150 °) is scarcely populated.

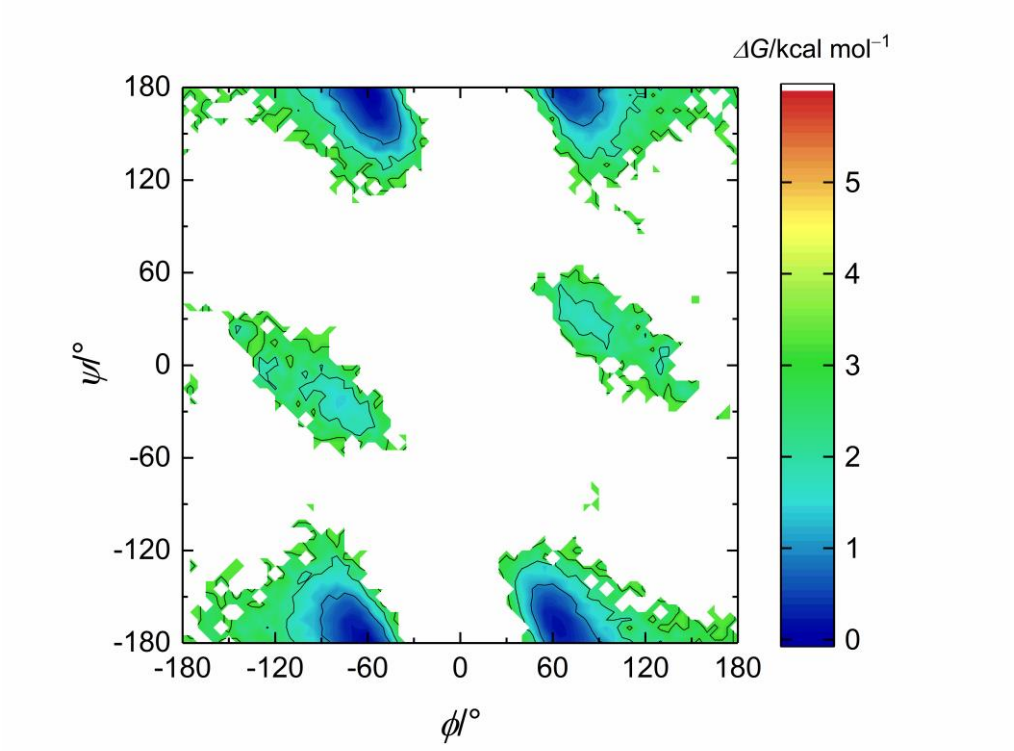

Figure S3. Relative Gibbs free energy contour map of the probability distribution of the Ramachandran (φ, ψ) angles of the central Gly residue of GGG zwitter-ion sampled during the last 100 ns of simulation in neat H_2O.

Dielectric relaxation of ternary solutions of triglycine (0.247 mol·L^{-1}) + water + salt

We fit the relaxation model described in eq. 1 of the main manuscript to all the experimental data for all salts used and all concentrations. The raw data with the corresponding fits are presented in Fig. S4 (and Fig. 2a of the main manuscript). From such fits we obtain the amplitudes and relaxation times of the triglycine and water relaxations, as well as the conductivity of each sample and the Cole-Cole parameter (α_{CC}) that describes the symmetric broadening of the loss peak of water. All the parameters are presented in the following figures (Figs. S5, S6 and S7).

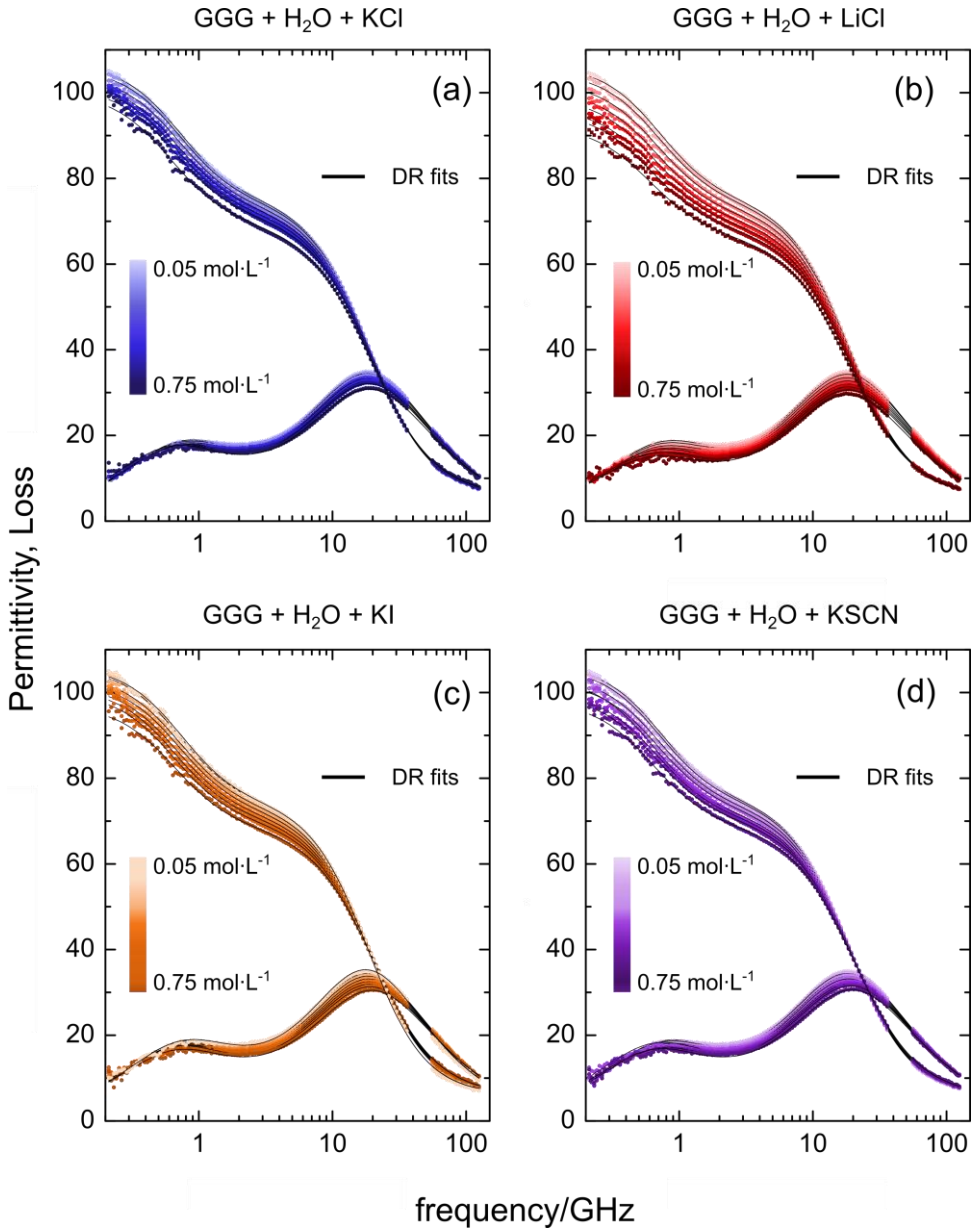

Figure S4. Complex permittivity spectra of mixtures of triglycine and water with increasing concentration (0.05, 0.10, 0.20, 0.30, 0.40, 0.50, 0.60, 0.75 mol·L^{-1}) of (a) KCl, (b) LiCl, (c) KI and (d) KSCN. The symbols correspond to experimental data and the solid lines show fits with the relaxation model described in eq. 1 (main manuscript). The Ohmic loss contribution (last term in eq. 1 has been subtracted for visual clarity).

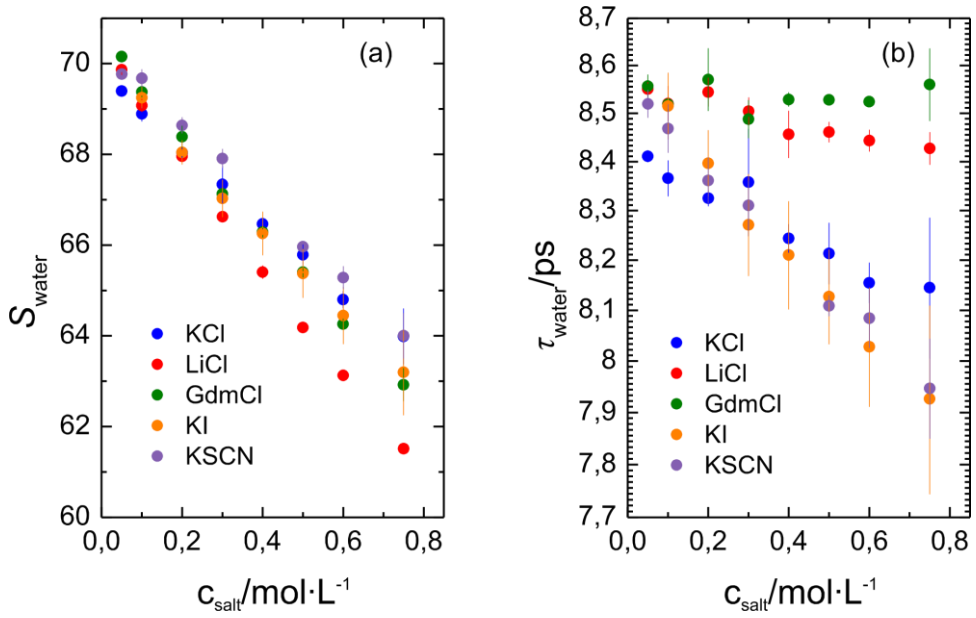

Figure S5. a) Amplitude (S_{water}) and b) relaxation time (τ_{water}) of the water relaxation versus salt concentration, as obtained from fitting eq.1 to the experimental data. The error bars correspond to the standard deviation of six independent measurements.

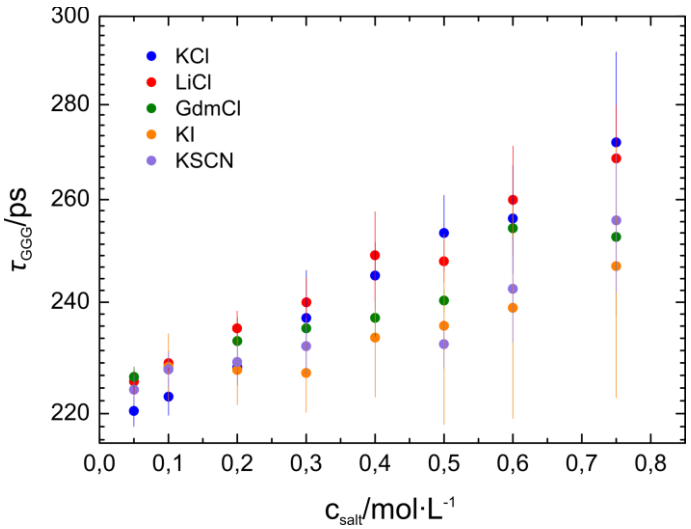

Figure S6. Relaxation time (τ_{GGG}) of the triglycine relaxation versus salt concentration, as obtained from fitting eq.1 to the experimental data. The error bars correspond to the standard deviation of six independent measurements.

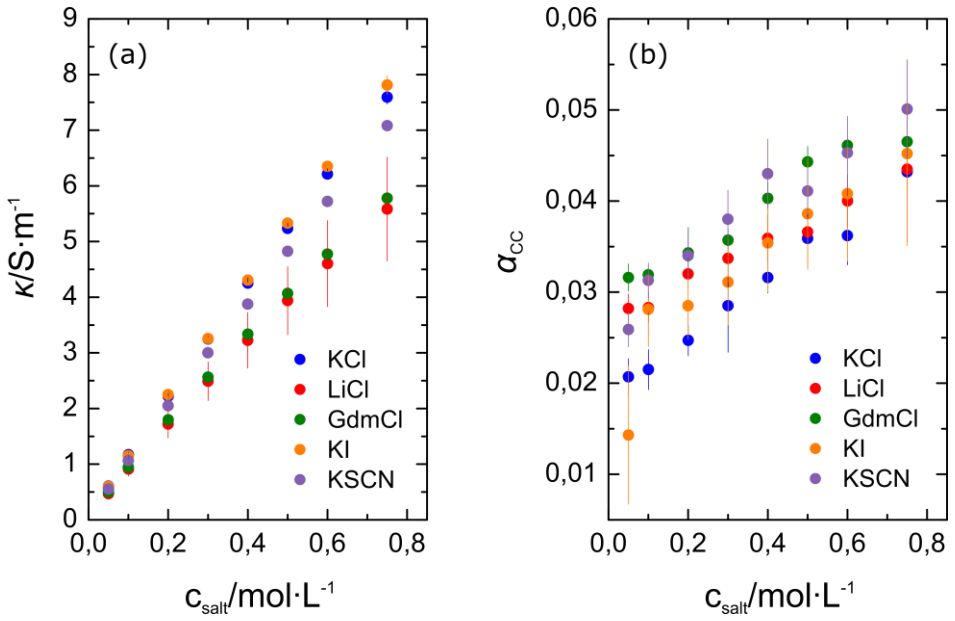

Figure S7. a) Conductivity (κ) and (b) Cole-Cole parameter (α_{CC}) versus salt concentration as obtained from fitting eq. 1 to the experimental data. The error bars correspond to the standard deviation of six independent measurements.

H-NMR measurements of triglycine (0.5 mg/mL) + D_2O + salt

To explore any contribution of specific association of ions to the charged termini of GGG, we performed NMR experiments on GGG in the presence of salts. As has been shown by others,[17] the variation of the chemical shift, δ, of GGG's CH_2 groups is very sensitive to the immediate environment of the CH_2 protons. For strong association of ions with GGG, the variation of the chemical shift with salt concentration, $\Delta\delta$:

$$\Delta\delta = \delta(c_{salt} = 0) - \delta\,(c_{salt}) \qquad \text{(S2)}$$

deviates from linearity. A linear variation of the chemical shift can be attributed to a continuous variation of the chemical environment (e.g. linear variation of the volume density of the molecules).[17] Also weak association equilibria lead to a rather linear variation of the chemical shift.[18] For strong binding (high corresponding association constants) NMR chemical shifts exhibit marked a non-linear variation with concentration. [17,18]

The determined values of $\Delta\delta$ of GGG protons for different salts are displayed in Fig. S7. As can be seen from this plot, the chemical shift of the CH_2 groups in the centre of the GGG molecule (position 2) and next to the carboxylate group (position 3) vary linearly with concentration. Hence, we find no evidence for long-lived contacts (strong association) between the studied salts and the amide groups and the carboxylate terminus, respectively. Only for the CH_2 group next to the N-terminus (position 1) $\Delta\delta(c_{\mathrm{salt}})$ somewhat deviated from linearity. However, these deviations neither correlate with the charge of the ions (cation or anion) nor with the nature of the ion. Hence, also from the CH_2 group near the NH_3^+ group we do not find evidence for significant association of ions to GGG. As such formation of long-lived "ion-pairs" are rendered unlikely based on the NMR chemical shift experiments.

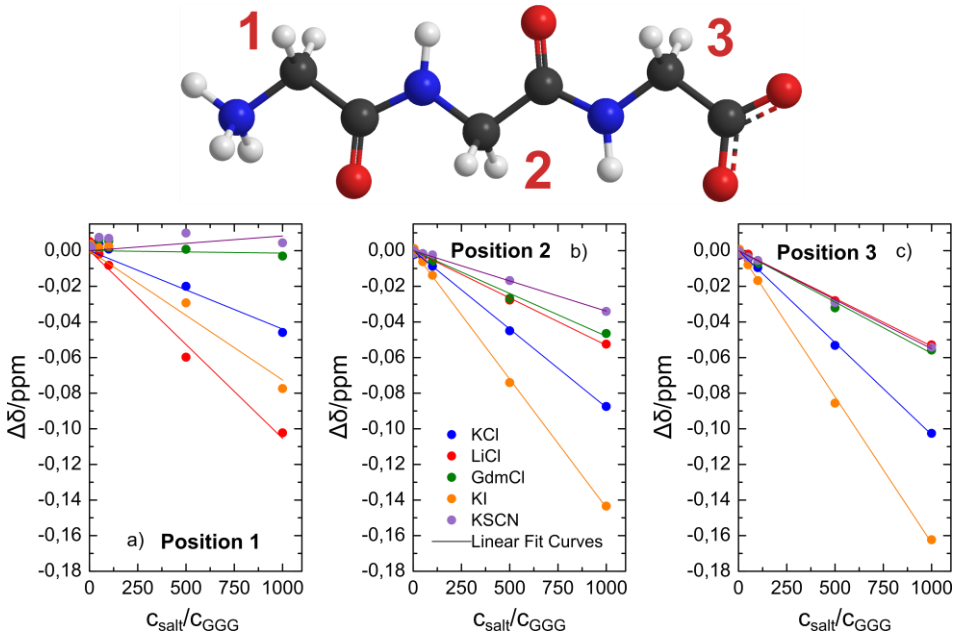

Figure S8. Top: Graphical representation of the GGG zwitterion marked with the positions of the CH_2 groups measured in the NMR. Bottom: Chemical shifts for the three CH_2 positions of GGG versus increasing molar ratios of GGG:salt. The solid lines correspond to best linear fit curves.

Supporting References

[1] W. Ensing, J. Hunger, N. Ottosson, H. J. Bakker, *J. Phys. Chem. C* **2013**, *117*, 12930–12935.

[2] E. A. S. Cavell, P. C. Knight, S. M. A., *Trans. Faraday. Soc* **1971**, *67*, 2225.

[3] J. C. Phillips, R. Braun, W. Wang, J. Gumbart, E. Tajkhorshid, E. Villa, C. Chipot, R. D. Skeel, L. Kalé, K. Schulten, *J. Comput. Chem.* **2005**, *26*, 1781–1802.

[4] J. Huang, S. Rauscher, G. Nawrocki, T. Ran, M. Feig, B. L. De Groot, H. Grubmüller, A. D. MacKerell, *Nat. Methods* **2016**, *14*, 71–73.

[5] R. B. Best, X. Zhu, J. Shim, P. E. M. Lopes, J. Mittal, M. Feig, A. D. MacKerell, *J. Chem. Theory Comput.* **2012**, *8*, 3257–3273.

[6] W. Humphrey, A. Dalke, K. Schulten, *J. Mol. Graph.* **1996**, *14*, 33–38.

[7] S. Bykov, S. Asher, *J. Phys. Chem. B* **2010**, *114*, 6636–6641.

[8] M. R. Shirts, D. L. Mobley, J. D. Chodera, V. S. Pande, *J. Phys. Chem. B* **2007**, *111*, 13052–13063.

[9] T. Darden, D. York, L. Pedersen, *J. Chem. Phys.* **1993**, *98*, 10089–10092.

[10] J. P. Ryckaert, G. Ciccotti, H. J. C. Berendsen, *J. Comput. Phys.* **1977**, *23*, 327–341.

[11] S. Miyamoto, P. A. Kollman, *J. Comput. Chem.* **1992**, *13*, 952–962.

[12] M. P. Allen, D. J. Tildesley, *Computer Simulation of Liquids*, Clarendon Press, **1989**.

[13] G. J. Martyna, D. J. Tobias, M. L. Klein, *J. Chem. Phys.* **1994**, *101*, 4177–4189.

[14] S. E. Feller, Y. Zhang, R. W. Pastor, B. R. Brooks, *J. Chem. Phys.* **1995**, *103*, 4613–4621.

[15] J. A. Drake, B. M. Pettitt, *J. Comput. Chem.* **2015**, *36*, 1275–1285.

[16] R. Schweitzer-Stenner, F. Eker, Q. Huang, K. Griebenow, *J. Am. Chem. Soc.* **2001**, *123*, 9628–9633.

[17] J. Paterová, K. B. Rembert, J. Heyda, Y. Kurra, H. I. Okur, W. R. Liu, C. Hilty, P. S. Cremer, P. Jungwirth, *J. Phys. Chem. B* **2013**, *117*, 8150–8158.

[18] L. Fielding, *Prog. Nucl. Magn. Reson. Spectrosc.* **2007**, *51*, 219–242.